

# Transparent ceramics for lighting

G.C. Wei

*Osram Sylvania, Beverly, MA, USA*

Available online 1 May 2008

## Abstract

The development of ceramic arc lamps for optical applications requires consideration of materials other than sintered polycrystalline alumina (PCA). Regular PCA is translucent, not transparent. Except small-grained, regular PCA cannot be used for high luminance applications such as required by projection systems. Silica lamps are currently operating close to their limit in highly loaded discharge lamps. These may be replaced with ceramic lamps so the Hg pressure may be elevated and/or higher powers achieved. Cubic materials can be polished to transparency for use as optical sources of short arcs. The current paper surveys the composition, structure, and properties of transparent ceramic lamp tube materials including small-grained PCA, sapphire, aluminum oxynitride, yttrium aluminate garnet, and dysprosium oxide. The challenges beyond the optical transparency are to achieve (1) strong bonding between the transparent ceramic and electrode system to complete the discharge enclosure, (2) satisfactory characteristics including thermo-mechanical properties in order to withstand the rapid heating and cooling cycles encountered in both the discharge tube and seal, (3) durability to resist the attack from lamp chemicals at high temperatures, and (4) stability to maintain the optical quality throughout the life. Performance, energy efficiency, environmental sustainability, and economics are driving the development of ceramic envelopes in lighting products. Transparent ceramics offer opportunities to push the limits of envelope materials for improved lamps. The paradigm used during the course of transparent ceramics research exemplifies advancement of new and improved materials.

© 2008 Elsevier Ltd. All rights reserved.

**Keywords:** Lamp envelopes; Oxides; Optical properties; Microstructure; Sintering

## 1. Introduction

Translucent polycrystalline alumina (PCA) doped with magnesia-based additives<sup>1</sup> discovered in 1960s has played an enabling role in the lighting industry. It made possible the construction and wide-spread use of high-pressure sodium lamps.<sup>2</sup> In 1990s, metal-halide lamps featuring translucent alumina tubes, cylindrical<sup>3</sup> or round,<sup>4</sup> were introduced for white-light, general-illumination applications, due to the nature of translucency (not transparency) of regular, translucent alumina. Regular PCA is translucent and its spectrophotometer in-line transmittance<sup>5</sup> is  $\sim 0.3$  compared to the overall total transmittance of  $\sim 0.98$ . Because of the scattering nature of this hexagonal material, regular PCA (unless small-grained) cannot be used for high luminance applications. If the arc tubes are transparent, the lamps could allow focused-beam applications such as projection lamps<sup>6</sup> and automotive headlights<sup>7</sup> containing various fills operating at temperatures higher than quartz. In

order to improve transparency or in-line transmittance, recent developments in PCA have made progress in two distinctly different directions of grain growth during sintering of PCA: (1) converting PCA to sapphire through abnormal grain growth, a solid-state crystal conversion (SSCC) process,<sup>8</sup> and (2) achieving transparent submicron-grained structure through sinter-HIP of compacts of nearly nano-size alumina powder.<sup>9</sup> Ceramics of cubic symmetry which limits birefringent light scattering at grain boundaries, are of interest due to their transparency in the polished state. These are AION,<sup>10</sup> YAG,<sup>11</sup>  $Y_2O_3$ ,<sup>12,13</sup> and  $Dy_2O_3$ .<sup>14</sup> The solubility of  $Y_2O_3$  in molten salts is high. Dysprosium oxide was tested because of reduced thermodynamic driving potentials for reactions with molten salt fills. Among the various applications (e.g. lamp envelope, optical lens/window, armor, infrared dome, and solid-state laser rod) for the transparent alumina and cubic ceramics with optical qualities comparable to single crystals of similar compositions, discharge tubes are the most demanding, because of the requirements of stability and durability of the transparent ceramics during high-temperature, steady-state plus on-and-off service involved in lamps.<sup>15</sup>

E-mail address: [george.wei@sylvania.com](mailto:george.wei@sylvania.com).

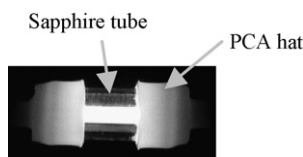


Fig. 1. Image of an operating sapphire-PCA-hat lamp<sup>7</sup>.

## 2. Experimental, results, and discussion

### 2.1. Sapphire

Straight sapphire tubes grown by melting and solidification have long been used in special lamps. A small layer of fine Mo precipitates (from dissolution of the Mo die in the molten alumina) along with pores caused by solidification shrinkage might be present in the near-surface region. If the levels of these defects are high, the total transmittance would be lower than those of regular PCA. Some recent designs of burners involved connection of straight sapphire tubes to PCA hats (Fig. 1).<sup>7,16</sup> The feedthrough scheme developed for PCA lamps<sup>3</sup> was utilized in the PCA hat.<sup>7</sup> The luminance of the sapphire burners was found to increase with increasing Ar pressure inside the discharge tube.<sup>7</sup> The microstructure of the sapphire-tube-PCA-hat interface is shown in Fig. 2. During formation of the interference bond, as PCA sintered and shrank upon sapphire, the initial sapphire-PCA boundary migrated towards PCA, sweeping across the original interface and leaving behind a string of voids (Fig. 2). The boundary motion (growth of sapphire into PCA), was similar to those reported in the literature.<sup>17</sup> In spite of anisotropy of sapphire with respect to PCA, the interface remained intact after thousands of on-and-off cycles in lamps.<sup>7</sup> This may be related to the relatively small sizes involved ( $\leq 9$  mm in diameter).

In the SSCC process,<sup>8</sup> the PCA doped with MgO was heat-treated to first achieve a state of equiaxed grain structure of translucency followed with out-diffusion of the MgO dopant to  $<60$  ppm so as to bring about a high rate of intrinsic grain growth to result in transparent sapphire shapes. The surface roughness and bulk residual pores of the PCA are typically preserved in the converted sapphire. It is challenging to achieve full conversion in large PCA parts consistently; oftentimes only surface region is converted. Examples of converted sapphire are shown

in Fig. 3. Strides<sup>8</sup> have been made with regard to the issues of the growth mechanism and conversion speed, which should assist in demonstration of the service of converted sapphire in lamps.

### 2.2. Small-grained alumina

PCA of submicron-grain-size and high in-line transmittance (very low residual porosity and small grains) was accomplished using sinter-HIP (hot isostatic pressing) of compacts consisting of nearly nano-size alumina particles.<sup>9</sup> The sealing structure developed for regular PCA metal halide lamps<sup>3</sup> can be readily used. The in-line transmittance in the visible range reached over 70% of that of sapphire. Computation of scattering and absorption indicated this was about the theoretical limit of the in-line transmittance for the grain size involved. The mechanical strength was as high as sapphire, due to the small grain size.<sup>9</sup> Such high-in-line transmittance, high strength, and ability of making into complex shapes (in contrast with anisotropy and straight tubes of melt-and-grown sapphire) made the material of interest for use as envelopes in beamers. Fig. 4 shows images of a fiber light-source placed inside the tubes, clearly demonstrating a better definition for the submicron-grained part versus regular, 15- $\mu$ m-grained alumina. The better image resolution is due to a relatively sharp curve of the angular dependence of the scattered light.<sup>9</sup>

For lamp envelope applications, it is important to have both high total and high in-line transmittance. Total transmittance, a measure of absorption, of arc tubes is critical to the total lumen output, while in-line transmittance which is mainly a measure of scattering is important to luminance (brightness) of the arc. A high in-line transmittance does not mean high total transmittance.<sup>5</sup> For example, very high-in-line sapphire tubes could have rather low total transmittance ( $<92\%$ ) caused by absorption due to Mo particles coming from slight dissolution of the Mo dies in the molten alumina and precipitation of Mo in the near-surface region of sapphire during solidification.

The total transmittance of the sub $\mu$ m-grained tubes was measured by placing a small light pipe (from a tungsten halogen lamp) inside the body, and measuring the total integrated flux of light passing the tube wall. The total transmittance values of as-sinter-HIPed discharge vessels were 77.7%, significantly lower than that (98–99%) of normal sintered alumina parts with 15  $\mu$ m grain size (Table 1). After annealing at 1025–1150 °C

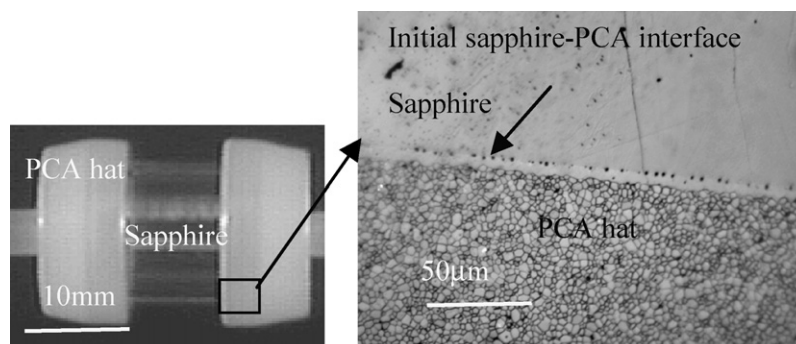


Fig. 2. Cross-section microstructure of sapphire-PCA interference bond.

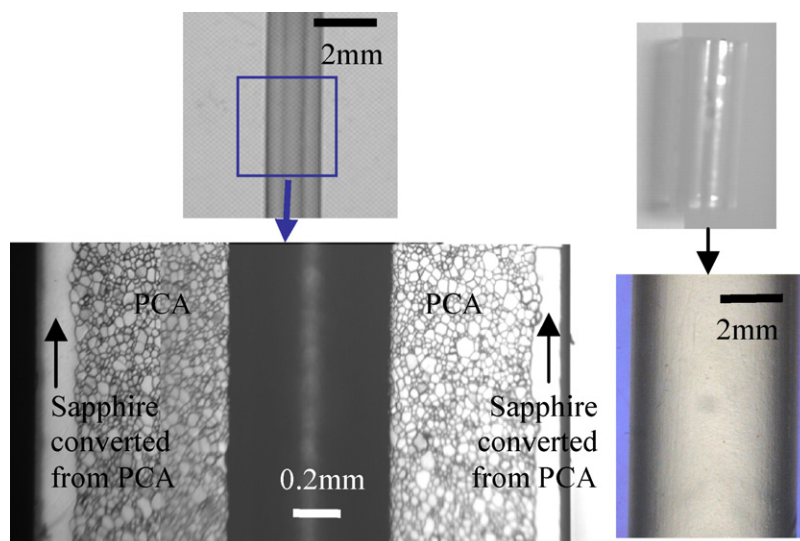


Fig. 3. Sapphire partially converted from MgO-doped PCA: cross-section microstructure showing complete conversion only in the near-OD region, left figures; outside views of nearly fully converted tubes showing retention of PCA surface ripples, right figures.

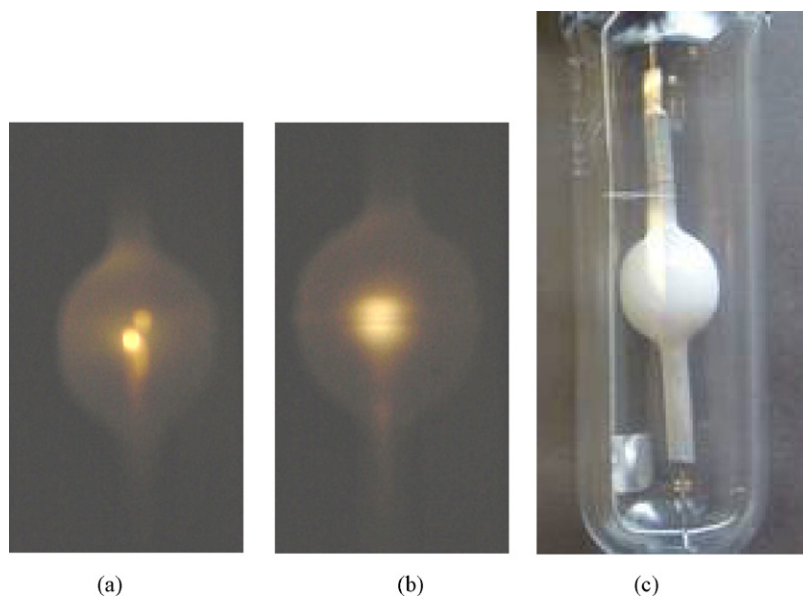


Fig. 4. Images of polished tubes containing fiber-optical miniature light source illustrating the relatively sharp image of the source in sub $\mu$ m PCA tube (a), vs. the diffuse image in regular PCA tube (b). One example of sub $\mu$ m PCA lamp is in (c).

in air for 2–4 h, the total transmittance of sub $\mu$ m-grained alumina vessels increased to 90.5%. Annealing under Ar–5 ppm  $O_2$  atmosphere at 1100 °C for 2 h increased the total transmittance of the sub $\mu$ m-grained discharge vessels to 95.0%. Some as-made tubes were faintly gray. Tubes annealed in air at 1025–1150 °C for 2–4 h had an added, undesirable, brownish hue which was observed in air-annealed PCA sintered in hydrogen. The sam-

ples became colorless after annealing under Ar–5 ppm  $O_2$ . The data clearly showed the benefits of post-sinter-HIP anneal in increasing the total transmittance to >92%, a level required for commercial lighting applications. The gray and brown discoloration appeared not related to metallic or carbon contamination, since various analyses such as bulk, surface, and cross-section techniques could not find any impurities significantly higher than

Table 1  
Total transmittance (%) of sub $\mu$ m-grained alumina tubes before and after annealing

	As-made	After anneal in air at 1025–1150 °C for 2–4 h	After anneal in Ar–5 ppm $O_2$ at 1100 °C for 2 h
Number of tube samples	18	18	18
Average total transmittance and standard deviation (%)	77.7 $\pm$ 6.8	90.4 $\pm$ 2.3	95.0 $\pm$ 1.8

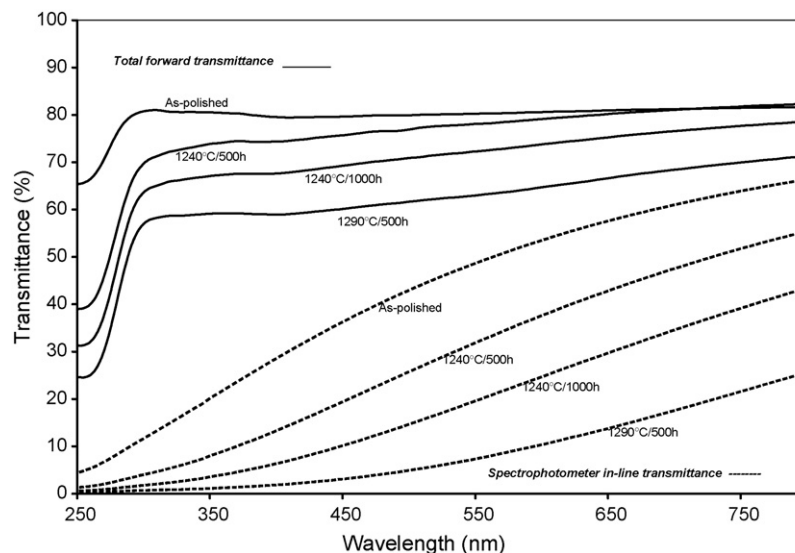


Fig. 5. Spectrophotometer total-forward and in-line transmittance vs. long-term temperature and time.

those in regular PCA. The discoloration is ascribed to color centers in PCA<sup>18</sup>: an oxygen vacancy with a trapped electron and an associated magnesium solute, a double oxygen vacancy with four trapped electrons, and an oxygen interstitial with two trapped holes, as explained in the following.

Sub $\mu\text{m}$ -grained alumina ceramics generally involves a higher level of MgO dopant to reach full density than larger-grained ( $\sim 15\ \mu\text{m}$ ) alumina based on micron-sized starting powders, because the nearly nano-sized powder requires higher MgO dopant to fully cover the surface of the finer, starting particles. Unlike the  $15\ \mu\text{m}$ -grained alumina, the MgO dopant ( $\sim 200$  to  $300\ \text{ppm}$ ) in sub $\mu\text{m}$ -grained alumina becomes completely dissolved in lattice and grain boundary region.<sup>15</sup> As a result, high levels of color centers are formed, which absorb light resulting in low total transmittance ( $\sim 77.7\%$ ) for the as-made MgO-doped, sub $\mu\text{m}$ -grained, alumina discharge vessels despite their very high in-line transmittance. The light-absorbing color centers were either converted or minimized such that the total transmittance increased during annealing under the specific  $\text{P}_{\text{O}_2}$ . The heat treatment temperature and time conformed to the temperature limit required for microstructural and transparency (in-line transmittance) stability.

In sub $\mu\text{m}$ -grained alumina doped with MgO sintering aid, growth of grains and pores occurred at temperatures as low as  $1150^\circ\text{C}$ .<sup>15</sup> At  $1240^\circ\text{C}$ , an average grain size of  $0.5\ \mu\text{m}$  grew to about  $1.1\ \mu\text{m}$  (Fig. 3), and the spectrophotometer transmittance (both total-forward and in-line) values at  $600\text{nm}$  dropped about 25–30% after 500 h at  $1240^\circ\text{C}$  (Fig. 5). Fig. 6 shows grain growth versus time at  $1150$ – $1290^\circ\text{C}$  in sub $\mu\text{m}$ -grained PCA, along with values reported in the literature.<sup>19,20</sup> Such grain-growth behavior is distinctly different from that of the regular,  $10$ – $30\ \mu\text{m}$ -grained PCA, which do not show any grain growth during 20,000 h service at  $\sim 1250^\circ\text{C}$  in HPS lamps. The observed grain growth at  $1150$ – $1290^\circ\text{C}$  is due to the extremely small size of the grains, since the grain growth rate is inversely proportional to the grain size.

The microstructural instability is tied to the solid solubility of MgO in alumina, which is a function of grain size in the range of sub $\mu\text{m}$  to  $\sim 2\ \mu\text{m}$ .<sup>21</sup> Electron microprobe mapping of the number density and sizes of  $\text{MgAl}_2\text{O}_4$  spinel particles of polished cross sections of samples annealed at  $1240^\circ\text{C}$  for 500 h is shown in Fig. 7. No spinel second phase was detected in as-sintered sub $\mu\text{m}$   $\text{Al}_2\text{O}_3$  doped with MgO. During sintering of compacts of MgO-doped, nearly nano  $\text{Al}_2\text{O}_3$  powders, the MgO dopant is all dissolved, in the lattice and grain-boundary region. During the subsequent heat treatment, grains and pores grow (Figs. 6–8) and  $\text{MgAl}_2\text{O}_4$  spinel precipitates out, while the enriched MgO level at grain boundaries, boundary width, and equilibrium MgO content in the lattice, undergo dynamic evolution, in a background of boundary motion, precipitation of second phase, and diffusional flux of the dopant. The decrease in transmittance and grain growth could also occur in small-grained PCA discharge tubes, which could become cloudy and exhibited grain growth after operation for thousands of hours in lamps (Figs. 9). The opaqueness in the arc tube could (1)

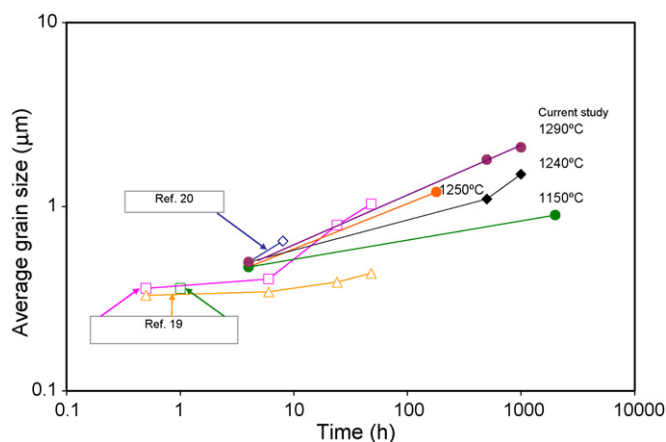


Fig. 6. Average grain size vs. time at various temperatures.



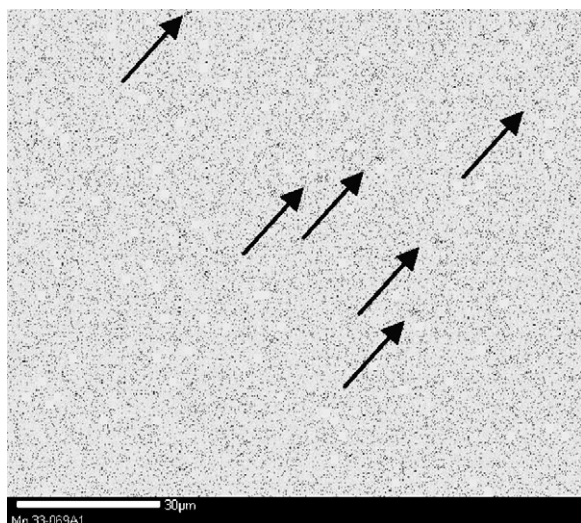


Fig. 7. Electron microprobe Mg mapping of sub $\mu$ m PCA annealed at 1240 °C for 500 h showing Mg-rich spots (indicated by arrows).

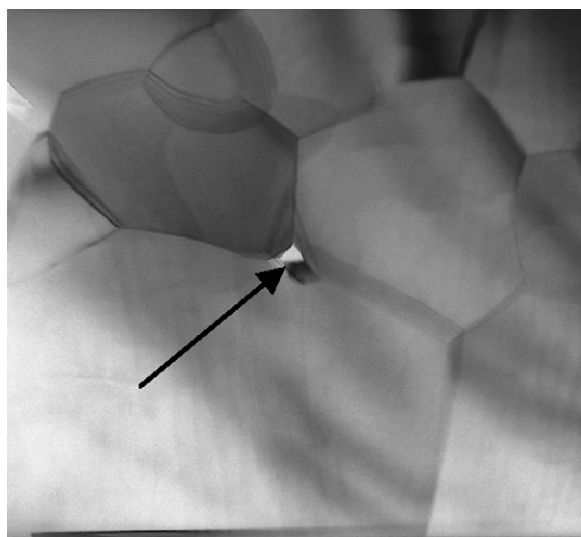


Fig. 8. Transmission electron micrograph of MgO-doped sub $\mu$ m PCA annealed at 1250 °C, showing pore growth (indicated by arrow).

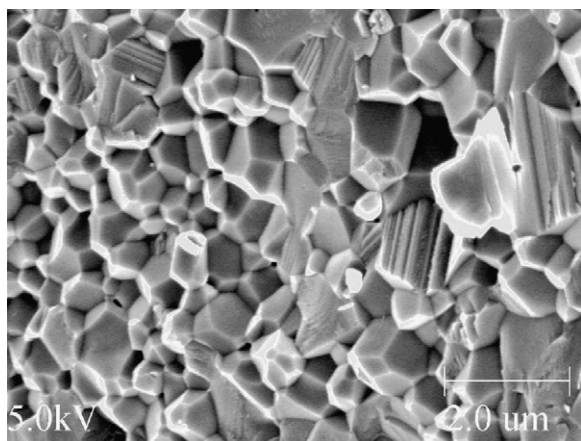


Fig. 9. Scanning electron micrograph of fractured surface of MgO-doped sub $\mu$ m PCA burner showing grain growth after operation in lamp for 500 h.

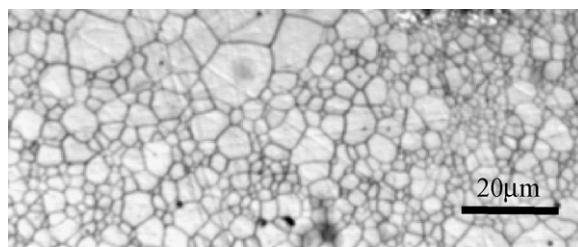


Fig. 10. Etched, polished optical micrograph of sintered YAG.<sup>27</sup>

increase emittance, which in turn, decrease lamp efficacy, and (2) increase reflectance to raise the wall temperature, which would further exacerbate grain growth and reactions of the wall with the fills. However, sub $\mu$ m-grained PCA was reportedly used in Hg–Tl–Na–In–I lamps with graded cermet and frit seals operating to 8000 h<sup>22</sup> with an unspecified wall temperature. Fills based on Dy–Tl–Na–Br–I were used in sub $\mu$ m-grained PCA lamps showing 78% maintenance at 1500 h.<sup>23</sup> The above cases suggested that the wall temperature of sub $\mu$ m-grained PCA tube would need to be carefully controlled in order to avoid degradation in transmittance and microstructure during service. An alternate strategy<sup>24</sup> was to maintain stability of the microstructure and in-line transmittance by increasing the grain size to 2  $\mu$ m with a sacrificial, broader angular dependence of scattering which might still be adequate for certain lamps.

### 2.3. AlON (aluminum oxynitride)

AlON ( $\text{Al}_{23}\text{O}_{27}\text{N}_5$ ) ceramic with cubic symmetry has been fabricated into excellent transparency in the visible.<sup>11</sup> The mechanical strength and thermal expansion of AlON are close to those of PCA,<sup>11</sup> so that AlON should be able to survive the stresses in ceramic metal halide lamps, and the end enclosure structure of PCA metal halide burners<sup>3</sup> can be utilized. In-line transmittance values in the visible as good as that of sapphire has been achieved in polished AlON ceramic.<sup>11</sup> However, thermodynamic calculations indicated that AlON was stable in a small range of  $\text{N}_2$  partial pressures at temperatures <1640 °C.<sup>25</sup> Another issue for use in projection lamps was the active oxidation behavior of AlON at temperatures  $\geq 1200$  °C in air.<sup>26</sup>

### 2.4. YAG (yttrium aluminate garnet)

Transparent YAG ceramic (yttrium aluminate garnet,  $\text{Y}_3\text{Al}_5\text{O}_{12}$ ) is of interest from the optical and mechanical properties standpoints.<sup>10</sup> It has cubic symmetry with an isotropic thermal expansion and no birefringence effect at the grain boundaries. Excellent transparency in the visible was achieved in YAG ceramic.<sup>10</sup> In addition to applications as host rods in solid-state lasers such as Nd-YAG,<sup>10(b),10(c)</sup> transparent YAG ceramics have been used as envelopes in lamps.<sup>15</sup> Because thermal expansion of YAG is very close to PCA, the feedthrough Scheme<sup>3</sup> developed for PCA lamps can be used for construction of YAG lamps. The microstructure of sintered YAG<sup>27</sup> derived from high-purity, finely divided YAG powder is shown in Fig. 10. Traces of residual phases such as  $\text{Y}_2\text{O}_3$  tend to give rise to exag-

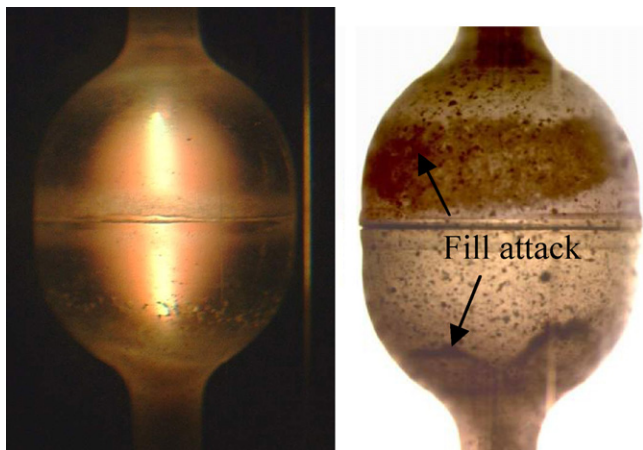
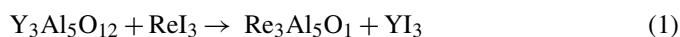


Fig. 11. Image of 2-piece YAG bulgy burner in operation (left figure), and after 1000 h showing “stains” or fill attack (right figure).

gerated grain growth. As predicted, the corrosion resistance of YAG to rare earth halide fills was less than that of PCA; the wall was attacked by the rare earth halide fills ( $\text{ReI}_3$ ) such as  $\text{TmI}_3$  after 1000 h, shown by the “stains” in the burner (Fig. 11) in accordance with the following reaction:



Yttrium emission lines were detected, color shifted, and voltage dropped in the YAG/ $\text{ReI}_3$  lamps (Fig. 11). Therefore, new, less corrosive fills are required for YAG lamps. There was no problem with thermal shock, as the YAG burners withstood many on-and-off lamp cycles.

### 2.5. Rare earth oxide ( $\text{Re}_2\text{O}_3$ )

Polycrystalline rare earth oxides such as dysprosium oxide are candidate tube materials for advanced beamers because of high transparency, low thermodynamic driving potentials for reactions with metal halide fills, satisfactory mechanical strength, and resistance to thermal shock.<sup>14</sup> Transparent polycrystalline  $\text{Dy}_2\text{O}_3$  ceramic parts were made by sintering of compacts of high-purity, finely-divided powders.<sup>28</sup>  $\text{Dy}_2\text{O}_3$  has a slight yellowish coloration due to intrinsic transitions. In spite of the slight yellowish coloration, the total transmittance is high ( $\sim 93\%$ ). The average grain size was  $\sim 3 \mu\text{m}$  (Fig. 12). Such small grain size is important as it imparts a high mechanical strength, because fracture strength of ceramics typically increases with decreasing flaw size, which in turn is controlled by grain size. The infrared cutoff wavelength ( $\sim 9 \mu\text{m}$ ) of  $\text{Dy}_2\text{O}_3$  is longer than that ( $\sim 6 \mu\text{m}$ ) of PCA due to the large atomic mass of  $\text{Dy}^{3+}$ , similar to the case ( $\sim 8.5 \mu\text{m}$ ) of  $\text{Y}_2\text{O}_3$ .<sup>11</sup> The long infrared cutoff suggested a lower emissivity and higher efficacy than PCA lamps. Fig. 13 shows room-temperature spectrophotometer in-line transmittance of  $\text{Dy}_2\text{O}_3$  disks. The  $\text{Dy}_2\text{O}_3$  has several intrinsic absorption bands in the range of 275–450 nm. The free energy of formation ( $-1514 \text{ kJ/mol}$ ) at 1200 K for  $\text{Dy}_2\text{O}_3$  is favorable, compared to those of  $\text{Al}_2\text{O}_3$  ( $-1295 \text{ kJ/mol}$ ) and  $\text{DyI}_3$  ( $-380 \text{ kJ/mol}$ ), and is nearly the same as that of  $\text{Tm}_2\text{O}_3$

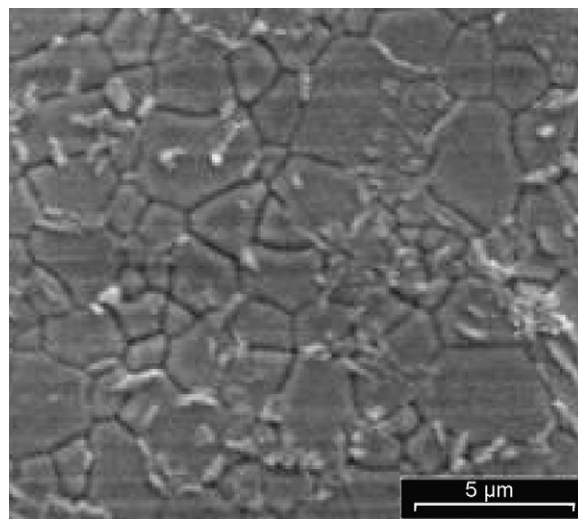


Fig. 12. Scanning electron micrograph of etched surface of  $\text{Dy}_2\text{O}_3$ .

( $-1526 \text{ kJ/mol}$ ),<sup>29</sup> suggesting stability of  $\text{Dy}_2\text{O}_3$  in the presence of the molten salts.

Fig. 14 shows one of the  $\text{Dy}_2\text{O}_3$  lamps containing  $\text{ReI}_3$  and Hg fills, in operation. The strong blue and UV absorption of the  $\text{Dy}_2\text{O}_3$  tube body filters some of the plasma radiation and alters the lamp color. The lamps properties were: 2500 K color temperature, 90 CRI and 84 lm/W. The performance was stable to at least 100 h. The hot spot was  $1143^\circ\text{C}$ .  $\text{Dy}_2\text{O}_3$  body absorbs the UV and blue radiation from Hg and rare earth emis-

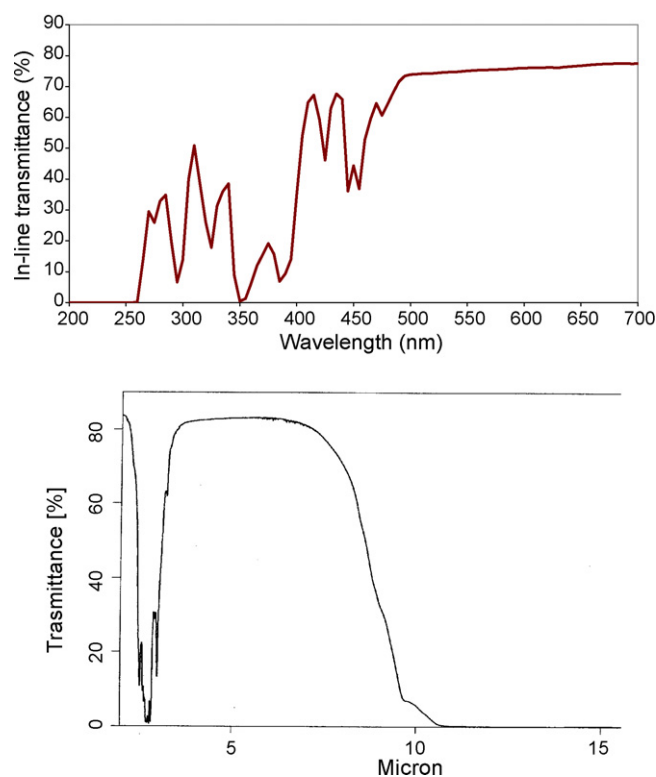


Fig. 13. Spectrophotometer in-line transmittance of polished  $\text{Dy}_2\text{O}_3$  (0.6mm thick) vs. wavelength: visible range (upper figure) and infrared range (lower figure).



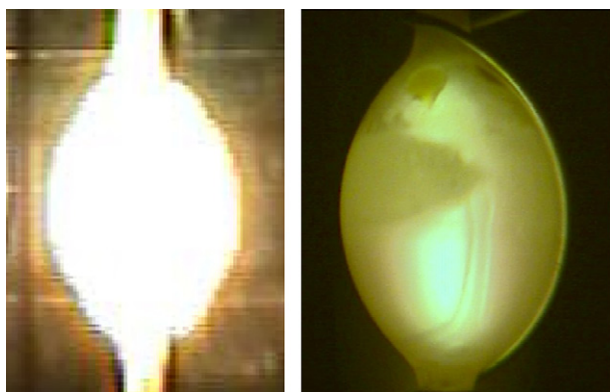


Fig. 14. Photographs of  $\text{Dy}_2\text{O}_3$  lamp in operation.

sion. This extra radiation, turned into heat, during run-up, gave rise to a rapid warm-up behavior.<sup>14</sup> In spite of calculated low thermodynamic driving force for reactions, some etching and corrosion occurred in lamps. Although the economic viability of the use of  $\text{Dy}_2\text{O}_3$  ceramic in improved lamps remains open, the above demonstrates that new transparent ceramic envelope materials can bring about opportunities for advanced high-intensity discharge projection systems.

### 3. Conclusions and summary

PCA envelopes have been essential to the construction of contemporary HPS and ceramic metal halide lamps in place of quartz. Studies have been conducted searching improved focused-beam light-sources using new transparent ceramic envelopes for higher wall temperatures, and better energy efficiency, color properties, and life. Many studies of producing new optical ceramics, involved sintering of ceramic materials to transparency for applications at lower temperatures or under less severe environments such as armor, window, infrared dome, and laser rod applications. Technological advancements in ceramic powder synthesis, forming, sintering and HIPing (hot isostatic pressing), have made possible a wide range of compositions (e.g. sub- $\mu\text{m}$ -grained  $\text{Al}_2\text{O}_3$ , YAG, AlON, and  $\text{Dy}_2\text{O}_3$ ), and shapes (cylindrical, bulgy, spherical, and elliptical), presenting significant flexibility to the designing of lamps and fill chemistry. It is important to understand both the advantages and limitations of each transparent ceramic, which need to be factored into consideration during lamp construction. The significant accomplishment in the optical properties of transparent ceramics resulted from improved understanding of powder-processing–microstructure–property inter-relationships. These transparent ceramics have in-line transmittance as high as quartz and higher than regular, translucent PCA. The challenges beyond the optical transparency are to achieve (1) strong bonding between the transparent ceramic and electrode system to complete the discharge enclosure, (2) satisfactory characteristics including thermo-mechanical properties in order to withstand the rapid heating and cooling cycles encountered in both the discharge tube and seal, (3) durability to resist the attack from lamp chemicals at high temperatures, and (4) stability to maintain the optical quality throughout the life. Performance, efficiency,

environmental sustainability, and economics are driving the development of ceramic envelopes in lighting products. Transparent ceramics offer opportunities to push the limits of envelope materials for improved lamps. The paradigm used during the course of transparent ceramics research exemplifies advancement of new and improved materials.

### Acknowledgements

The author would like to acknowledge many individuals who have provided input to various aspects of transparent ceramic research, in particular: M. Harmer (Lehigh University), A. Krell (IKTS), and colleagues at Osram Sylvania & Osram.

### References

1. Coble, R. L., Sintering crystalline solids: I. Intermediate and final stage diffusion models; II. Experimental test of diffusion models in powder compacts. *J. Appl. Phys.*, 1961, **32**, 787–799.
2. de Groot, J. J. and van Vliet, J., *The high-pressure sodium lamp*. Macmillan, London, 1986.
3. Seinen, P. A., High intensity discharge lamp with ceramic envelopes; a key technology for the lighting future. In *Proc. 7th Int. Sym. Sci. & Tech. of Light Sources*, 1995, pp. 101–109.
4. Juengst, S., Lang, D. and Galvez, M., Arc tubes for improved isothermal operation. In *Proc. 10th Int. Sym. Sci. & Tech. of Light Sources*, 2004, pp. 115–124.
5. Wei, G., Characterization of translucent polycrystalline alumina ceramics. *Cer. Trans.*, 2002, **133**, 135–144.
6. Kappen, T., Ceramic metal halide lamps; a world of lighting. In *Proc. 10th Int. Sym. Sci. & Tech. of Light Sources*, 2004, pp. 43–52.
7. Guenther, K., Hartmann, T. and Sarroukh, H., Hg-free ceramic automotive headlight lamps. In *Proc. 10th Int. Sym. Sci. & Tech. of Light Sources*, 2004, pp. 219–220.
8. (a) Scott, C., Kaliszewski, M., Greskovich, C. and Levinson, L., Conversion of polycrystalline  $\text{Al}_2\text{O}_3$  into single-crystal sapphire by abnormal grain growth. *J. Am. Ceram. Soc.*, 2002, **85**, 1275–1280; (b) Thompson, G., Harmer, M., Henderson, P., Wei, G. and Rhodes, W., Conversion of polycrystalline alumina to single-crystal sapphire by localized doping with silica. *J. Am. Ceram. Soc.*, 2004, **87**, 1879–1882; (c) Greskovich, C. and Brewer, J., Grain-boundary migration at high velocity in  $\text{Al}_2\text{O}_3$ . *J. Am. Ceram. Soc.*, 2007, **90**, 1375–1381; (d) Dillon, S. J. and Harmer, M. P., Mechanism of solid state single crystal conversion in alumina. *J. Am. Ceram. Soc.*, 2007, **90**, 993–995.
9. (a) Hayashi, K., Kobayashi, O., Toyoda, S. and Morinaga, K., Transmission optical properties of polycrystalline alumina with submicron grains. *Mater. Trans. JIM*, 1991, **32**, 1024–1033; (b) Krell, A., Blank, P., Ma, H., Hutzler, T., van Bruggen, M. P. B. and Apetz, R., Transparent sintered corundum with high hardness and strength. *J. Am. Ceram. Soc.*, 2003, **86**, 12–18; (c) Apetz, R. and van Bruggen, M., Transparent alumina: a light scattering model. *J. Am. Ceram. Soc.*, 2003, **86**, 480–486; (d) Krell, A., Hutzler, T. and Klimke, J., Transparent ceramics for structural applications: part I: physics of light transmission and technological consequences, part II: fields of applications. *Ceram. Forum Inter./Ber. DGK*, 2007, **84**(4), E41–E50; Krell, A., Hutzler, T. and Klimke, J., Transparent ceramics for structural applications: part I: physics of light transmission and technological consequences, part II: fields of applications. *Ceram. Forum Inter./Ber. DGK*, 2007, **84**(6), E50–E56.
10. (a) de With, G. and van Dijk, H., Translucent  $\text{Y}_3\text{Al}_5\text{O}_{12}$  ceramics. *Mater. Res. Bull.*, 1984, **19**, 1669–1674; (b) Ikesue, A., Kinoshita, T., Kamata, K. and Yoshida, K., Fabrication and optical properties of high-performance polycrystalline Nd:YAG ceramics for solid-state lasers. *J. Am. Ceram. Soc.*, 1994, **78**, 1033–1040;

- (c) Yanagitani, T., Imagawa, S., Yagi, H., and Kubo, H., A corrosion resistant ceramic and a production method thereof, *Euro. Patent No.* EP0926106A1, 1998.
11. (a) McCauley, J. M. and Corbin, N. D., Phase relations and reaction sintering of transparent cubic aluminum oxynitride (AlON) spinel. *J. Am. Ceram. Soc.*, 1979, **62**, 476–479;  
(b) Hartnett, T. M. and Gentilman, R. L., Optical and mechanical properties of highly transparent spinel and AlON domes. *Proc. SPIE*, 1984, **505**, 15–22.
  12. Greskovich, C. and Chernoch, J., Polycrystalline ceramic lasers. *J. Appl. Phys.*, 1973, **44**, 4599–4606.
  13. Rhodes, W., Controlled transient solid second-phase sintering of yttria. *J. Am. Ceram. Soc.*, 1981, **64**, 13–19.
  14. Wei, G., Lapatovich, W. and Browne, J., Dysprosium oxide ceramic arc tube for HID lamps. In *Proc. 11th Int. Sym. Sci. & Tech. of Light Sources*, 2007, pp. 559–560.
  15. Wei, G., Transparent ceramic lamp envelope materials. *J. Phys. D. Appl. Phys.*, 2005, **38**, 3057–3065.
  16. Wei, G., Kramer, J., Walsh, J., and Lapatovich, W., Arc tube for electrodeless lamp, *US Patent No.* 5621275, 1997.
  17. Monahan, R. D. and Halloran, J. W., Single-crystal boundary migration in hot-pressed aluminum oxide. *J. Am. Ceram. Soc.*, 1979, **62**, 564–567.
  18. Brock, L., Raukas, M., Mishra, K., Lapatovich, W. and Wei, G., Color centers in MgO-doped polycrystalline alumina. *MRS Proc. Lumin. Lumin. Mater.*, 2001, **667**, G7.1.1–11.
  19. Yeh, T. and Sacks, M., Low-temperature sintering of aluminum oxide. *J. Am. Ceram. Soc.*, 1988, **71**, 841–844.
  20. Xue, L. and Chen, I., Deformation and grain growth of low-temperature-sintered high-purity alumina. *J. Am. Ceram. Soc.*, 1990, **73**, 3518–3521.
  21. Wei, G., Sintering and grain growth in polycrystalline alumina. *J. Cer. Soc. Jpn.*, 2004, **112**, S179–S182.
  22. Nagayama, H., Structure of sealing part of arc tube and method of manufacturing the same, *Euro. Patent application No.* EP0650184A1, 1995.
  23. Yagi, H., Yamazaki, H., and Kubo, H., A high-purity alumina ceramic and its manufacturing method, *Jpn. Patent No.* JP2001-199761, 2001.
  24. (a) Watanabe, K., Translucent ceramic envelopes for HID lamps. In *Proc. 11th Inter. Light Source Symp. (LS:11)*, 2007, pp. 89–92;  
(b) van Bruggen, M., Kop, T., and Keursten, T., Transparent polycrystalline aluminum oxide, *US Patent No.* 2006/0169951.
  25. Willems, H. X., Hendrix, M., Metselarr, R. and de With, D., Thermodynamics of AlON I: stability at lower temperatures. *J. Eur. Ceram. Soc.*, 1992, **10**, 327–337.
  26. Willems, H. X., Preparation and properties of translucent  $\gamma$ -aluminum oxynitride, Thesis, Tech Univ. Eindhoven, 1992, 29–30.
  27. Wei, G., Transparent polycrystalline yttrium alumina garnet, *US Patent No.* 6844285, 2004.
  28. Yagi, H. and Yanagitani, T., Translucent rare earth oxide sintered article and method for production thereof, *Euro. Patent No.* EP1336596, 2002.
  29. Barin, I., *Thermochemical data*. VCH Weinheim, Germany, 1993.